Publication I

Eero Tölö, Juha Suorsa, and Ari Harju. 2008. Two interacting electrons in a square quantum dot. Physica E, volume 40, number 5, pages 1038-1041.

Available online at www.sciencedirect.com
ScienceDirect
Physica E 40 (2008) 1038–1041
PHYSICA E
www.elsevier.com/locate/physe

Two interacting electrons in a square quantum dot

Eero Tölö, Juha Suorsa, Ari Harju*

Laboratory of Physics, Helsinki University of Technology, P.O. Box 4100, FIN-02015 HUT, Finland

Available online 29 September 2007

Abstract

Properties of a two-electron, square quantum dot are studied using the exact diagonalization method. The emphasis is on the analysis of the conditional wave function, showing a vortex structure formation at strong magnetic fields. We find that additional vortices in the system are generated by splitting of the antisymmetry generating vortices (Pauli-vortices).

PACS: 73.21.La; 71.10.Pm

Keywords: Quantum dots; Vortices

1. Introduction and model

A commonly used, non-parabolic, model for a semiconductor quantum dot [1] (QD) is a square, hard-wall QD, see e.g. Refs. [2–14]. The enhanced magnetic field and correlation effects in quasi-two-dimensional semiconductor quantum systems give rise to interesting properties even in small systems like two-electron QD [15–17]. In this paper we study two interacting electrons in a square QD. One of the aims of this paper is to study the magnetic field induced vortex formation in this system [18].

The model Hamiltonian of a two-electron QD system can be written as

$$H = \sum_{i=1}^{2} \left[\frac{(\mathbf{p}_i + e\mathbf{A}_i/c)^2}{2m^*} + V_{\mathrm{ext}}(\mathbf{r}_i) \right] + C \frac{e^2}{\varepsilon |\mathbf{r}_1 - \mathbf{r}_2|}, \tag{1}$$

where the electrons are restricted to the xy plane. The ambient bulk medium gives rise to an effective mass m^* and dielectric constant ε, for GaAs $m^* = 0.067 m_e$ and $\varepsilon = 12.7$. We include an extra dimensionless parameter C which parametrizes the strength of interactions between the electrons, with the natural strength obtained at $C = 1$. While the effective strength of the interaction could also be tuned by changing the size of the system, scaling C is more transparent as it keeps the magnetic flux the same. The magnetic field $\mathbf{B} = B\mathbf{u}_z$ perpendicular to the xy plane is included using the symmetric gauge $\mathbf{A} = -B/2(y\mathbf{u}_x - x\mathbf{u}_y)$. We use a hard-wall external potential V_{ext} with equal side lengths, taken to be 2π in effective atomic units, which corresponds to a length of order 60 nm.

We expand the finite magnetic field, interacting wave function in a basis of non-interacting states of the zero magnetic field value, taking both the interaction and the magnetic field as perturbations on the system. The Hamiltonian matrix elements of the $\mathbf{A}$ dependent terms are calculated analytically, whereas the interaction matrix elements are computed numerically from a two-dimensional integral, obtained by expressing $1/|\mathbf{r}_1 - \mathbf{r}_2|$ in terms of its Fourier transform. We use from 64 to 112 single-particle spatial orbitals, and obtain the lowest many-body eigenstates by Lanczos diagonalization.

Due to lack of $O(2)$ symmetry, the z-component of angular momentum is not conserved in our model. However, the system has a 4-fold rotational symmetry C_4, and an angular Bloch momentum can be introduced [19]. If one expands the interacting many-body wave function using the eigenfunctions of the angular momentum, one can see that the Hamiltonian couples states that have angular momentum values differing by a multiple of four. In general, an n-fold rotational symmetry couples states that differ by a multiple of n. Taking $n \to \infty$, the

*Corresponding author. Tel.: +358 9 451 5811; fax: +358 9 451 3241.
E-mail address: ari.harju@hut.fi (A. Harju).

1386-9477/$ - see front matter
doi:10.1016/j.physe.2007.09.133

$O(2)$ symmetry is recovered as the coupling between different angular momentum eigenstates vanishes. The results below for the C_4 case are interesting as being close to the opposite limit.

2. Results

The two lowest energy levels of the two-electron QD as a function of C and B are shown in Fig. 1. For $C \neq 0$ the states show regular crossing behavior. One can see that in the limit of strong interactions, the two lowest states approach each other and also more crossings can be seen. The difference of the two lowest energies form a clear diamond-shaped structure. The total spin of the system changes at each change of the ground state. The general reasoning for this type of behavior is that the magnetic field squeezes the system up to a point where it is energetically favorable for the system to expand. The price to pay for the lowered interaction energy is the increased kinetic energy. As the particles at strong magnetic field do cyclotron motion, the increased kinetic energy corresponds to an increased radius and also to an increased magnetic field flux inside the cyclotron orbit.

In Fig. 2 we show the ground state expectation value of the angular momentum as a function of the interaction strength. Even though the angular momentum is not a good quantum number, a clear staircase structure is seen. For weak interaction values the deviation from integer values is marginal and each plateau is very flat. This is not the case for the strongly interacting system. The reason for the difference in these cases is that in the weakly interacting dot the electrons are rather close to the center of the dot, feeling the corners only marginally, and due to this the system is nearly circularly symmetric. In the strongly interacting limit the electrons tend to localize on opposite corners of the dot, removing the circular symmetry.

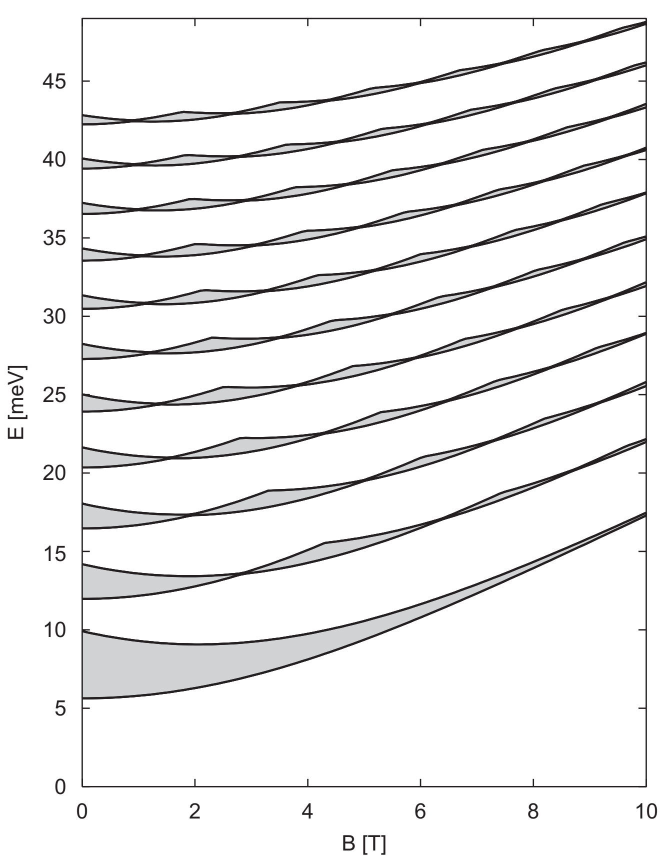

Fig. 1. Two lowest eigenenergies for interaction strengths $C = 0, 1, \ldots, 10$. The gray shading joins energies with the same C. The spin of the system changes at each crossing of the eigenenergies, being zero at zero magnetic field.

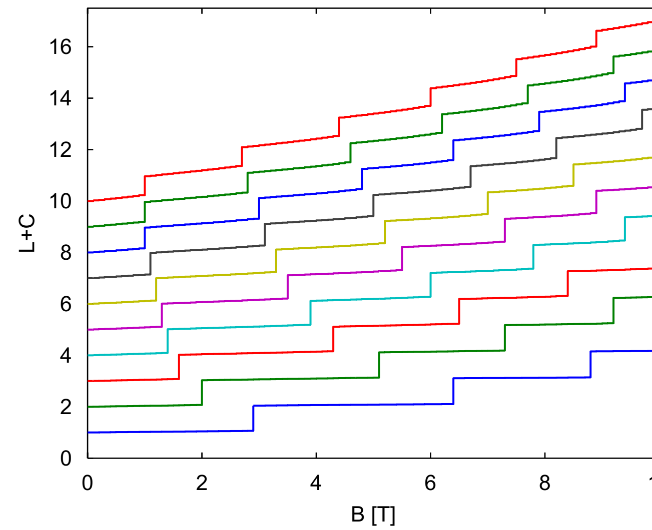

Fig. 2. The expectation value of angular momentum L as a function of magnetic field B for interaction strengths $C = 1, 2, \ldots, 10$. The L-values are shifted by C for clarity. Clear plateaus are seen even for the strongly interacting cases.

Further information on the system can be obtained from the conditional wave function, constructed in the following way: we first find the most probable electron positions $\{\mathbf{r}_i^*\}_{i=1}^2$ by maximizing the density $|\Psi|^2$. Then one of the electrons is moved to a new position $\mathbf{r}$, and a conditional single-particle wave function is evaluated as

$$\psi_c(\mathbf{r}) = \frac{\Psi(\mathbf{r}, \mathbf{r}_2^*)}{\Psi(\mathbf{r}_1^*, \mathbf{r}_2^*)}.$$

The change in the phase can be obtained from the angle θ of the wave function $\psi_c(\mathbf{r}) = |\psi_c(\mathbf{r})| \exp(i\theta(\mathbf{r}))$. One should note that the mere phase is not a real physical observable; however, real physical information can be obtained by examining the phase along loops. The first set of ψ_c's is shown in Fig. 3. In Fig. 3(a) one can see that the most probable positions of the electrons are on opposite corners of the dot. The conditional density is somewhat localized on the upper-left corner, and the phase of the conditional wave function is constant. In Fig. 3(b) the system is spin-polarized and one can see a Pauli-vortex on top of the fixed electron on the lower-right corner. We call this vortex a Pauli-vortex as it leads to antisymmetry of the space part of the wave function, and ensures the Pauli exclusion principle at finite magnetic field. Increasing the magnetic field

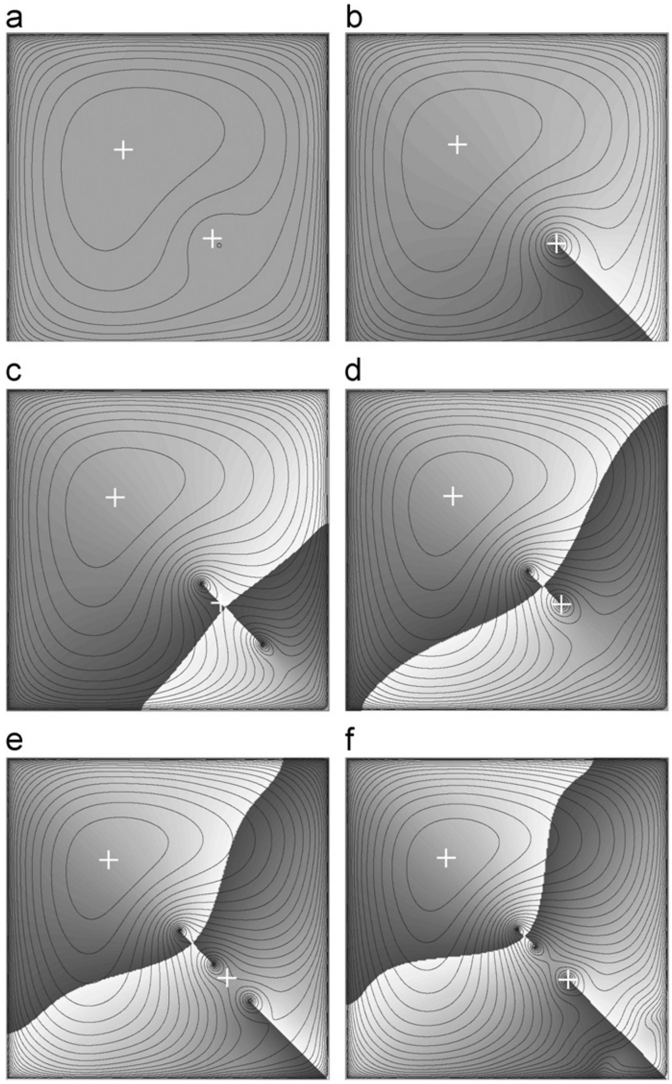

Fig. 3. Most probable electron positions $\{\mathbf{r}_i^*\}_{i=1}^N$ (plusses) and conditional electron densities (contours) and phases (gray-scale). We probe with the leftmost electron and densities are on logarithmic scale. The phase changes from π to $-\pi$ on the lines where shadowing changes from darkest gray to the white. The interaction strength C is one, and panels from (a) to (f) are for magnetic field values of $B = 1, 4, 7, 10, 11$ and $13\,\mathrm{T}$, correspondingly. The left panels correspond to $S = 0$ and right ones have $S = 1$.

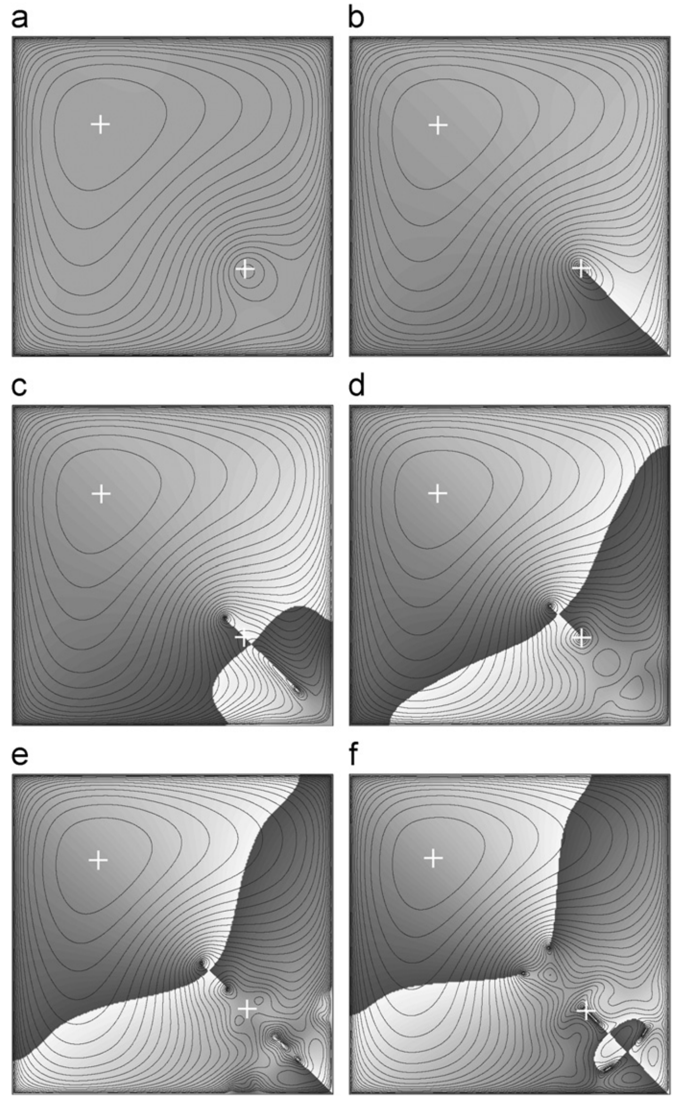

Fig. 4. Same as Fig. 3 but for interaction strength $C = 5$. Magnetic field values are $B = 1, 3, 5, 7, 7.5$ and $8.5\,\mathrm{T}$.

further to 7 T, the ground state switches back to $S = 0$, and instead of a Pauli vortex, two vortices can now be seen close to the fixed electron in Fig. 3(c). At 10 T shown in Fig. 3(d), one can still see two vortices, but now one of them is a Pauli-vortex. The system has again $S = 1$. Finally, at Figs. 3(e) and (f) one can see three vortices, the difference being that in (f) one of the vortices is a Pauli-vortex.

From Fig. 3 it can be seen that the additional vortices are generated by splitting of the Pauli-vortex into two vortices. In the next step, one of these vortices changes to a Pauli-vortex, which again splits in the next step. One should note that in the two-electron parabolic dot the center-of-mass and relative motion decouple and one can easily find that in that case the vortices are always found on top of the second electron and no vortex splitting is seen. The way the vortices are generated also explains the plateaus of the angular momentum, as the vortices do not continuously penetrate to the system from the sides, as is the case in the QD molecule [17], but are generated by a Pauli-vortex splitting.

The conditional wave functions of a more strongly interacting system, with $C = 5$, are shown in Fig. 4. While the localizing effect of the interaction is more pronounced than in the $C = 1$ case, the generation of vortices follows the same rule as was found for the $C = 1$ case above.

3. Conclusions

We have studied two interacting electrons in a square QD, and found periodic crossings of the two lowest eigenenergies as a function of the applied magnetic field. We found an approximate angular momentum quantization which is non-trivial for a system lacking circular symmetry. Our analysis of the ground state wave function shows that the magnetic field induces regular vortices on the system, generated by splitting of the Pauli-vortices attached to electrons. As the vortices carry quantized angular momentum, the abrupt birth of vortices naturally explains the plateaus and jumps of the angular momentum.

Acknowledgments

We thank Yvette Hancock for careful reading of the manuscript. This work has been supported by the Academy of Finland through its Centers of Excellence Program (2006–2011).

References

[1] L. Jacak, P. Hawrylak, A. Wójs, Quantum Dots, Springer, Berlin, 1998.
[2] G.W. Bryant, Phys. Rev. Lett. 59 (1987) 1140.
[3] W. Sheng, H. Xu, Physica B 256–258 (1998) 152.
[4] C.E. Creffield, W. Häusler, J.H. Jefferson, S. Sarkar, Phys. Rev. B 59 (1999) 10719.
[5] R. Ugajin, Phys. Rev. B 51 (1995) 10714.
[6] R. Ugajin, Phys. Rev. B 53 (1996) 6963.
[7] C.E. Creffield, J.H. Jefferson, S. Sarkar, D.L. Tipton, Phys. Rev. B 62 (2000) 7249.
[8] S. Akbar, I.-H. Lee, Phys. Rev. B 63 (2001) 165301.
[9] M. Valín-Rodríquez, A. Puente, L. Serra, Phys. Rev. B 64 (2001) 205307.
[10] L.G. Dias da Silva, M.A. de Aguiar, Phys. Rev. B 66 (2002) 165309.
[11] E. Räsänen, H. Saarikoski, M.J. Puska, R.M. Nieminen, Phys. Rev. B 67 (2003) 035326.
[12] E. Räsänen, H. Saarikoski, V.N. Stavrou, A. Harju, M.J. Puska, R.M. Nieminen, Phys. Rev. B 67 (2003) 235307.
[13] E. Räsänen, A. Harju, M.J. Puska, R.M. Nieminen, Phys. Rev. B 69 (2004) 165309.
[14] M. Novaes, M.A.M. de Aguiar, Phys. Rev. E 70 (2004) 045201.
[15] A. Harju, S. Siljamäki, R.M. Nieminen, Phys. Rev. Lett. 88 (2002) 226804.
[16] M. Marlo, A. Harju, R.M. Nieminen, Phys. Rev. Lett. 91 (2003) 187401.
[17] M. Helle, A. Harju, R.M. Nieminen, Phys. Rev. B 72 (2005) 205329.
[18] H. Saarikoski, A. Harju, M.J. Puska, R.M. Nieminen, Phys. Rev. Lett. 93 (2004) 116802.
[19] A. Ferrando, Phys. Rev. E 72 (2005) 036612.